

Supplementary Table 2

	Control mice	GMCSFR $\beta$ KO mice
Lavaged lung unlabelled PC (nmoles/g)	50.94 $\pm$ 5.72	149.76 $\pm$ 21.68
Lavaged lung <i>methyl</i> -D <sub>9</sub> -choline labelled PC (nmoles/g)	0.96 $\pm$ 0.10	0.70 $\pm$ 0.07
BALF unlabelled PC (nmoles/100 $\mu$ l)	107.07 $\pm$ 12.06	400.28 $\pm$ 91.76
BALF <i>methyl</i> -D <sub>9</sub> -choline labelled PC (nmoles/100 $\mu$ l)	1.74 $\pm$ 0.44	0.27 $\pm$ 0.06

**Supplementary Table 2:** Comparison of *methyl*-D<sub>9</sub>-choline labelling of PC from control and GMCSFR $\beta$  KO mouse lavaged lung and corresponding BALF samples. PC content was determined in extracts of lungs and BALF from 12 week old animals (n=5, means  $\pm$  SD) labelled with *methyl*-D<sub>9</sub>-choline for 5h. Dilution of labelled PC within the elevated pool sizes of unlabelled PC in both GMCSFR $\beta$  KO lungs and BALF relative to control animals explain the large decrease in labelling enrichments seen in Figures 6c and 6f.

**Chronic pharmacological antagonism of the GM-CSF receptor in mice does not replicate the pulmonary alveolar proteinosis (PAP) phenotype but does alter lung surfactant turnover.**

Dominic J Corkill<sup>1</sup>, Alan N Hunt<sup>2</sup>, Mary Jane Hinrichs<sup>3</sup>, Nicholas White<sup>4</sup>, Marlon Rebelatto<sup>3</sup>, Lorin Roskos<sup>3</sup>, Josquin Nys<sup>1</sup>, Alison Scott<sup>5</sup>, Matthew J Robinson<sup>1</sup>, Patricia Ryan<sup>3</sup>, Anthony D Postle<sup>2</sup>, Matthew A Sleeman<sup>1</sup>

<sup>1</sup>Research and Early Development, Respiratory & Immunology (R&I), AstraZeneca, Cambridge UK; <sup>2</sup>Clinical & Experimental Sciences, Faculty of Medicine, University of Southampton, Southampton SO16 6YD; <sup>3</sup>Biologics Safety Assessment, AstraZeneca, Gaithersburg, USA; <sup>4</sup>Bioanalytical Sciences, AstraZeneca, Cambridge, UK; <sup>5</sup>Biologics Safety Assessment, AstraZeneca, Cambridge, UK;

**Corresponding Author:**

Dr Alan N Hunt

Clinical & Experimental Sciences  
Faculty of Medicine  
Room LF75, Level F, South Block,  
Southampton General Hospital  
Tremona Road  
Southampton SO16 6YD  
United Kingdom

Email [anh@soton.ac.uk](mailto:anh@soton.ac.uk)

## Abstract

Granulocyte macrophage colony stimulating factor (GM-CSF) is a key participant in, and a clinical target for, the treatment of inflammatory diseases including rheumatoid arthritis (RA). Therapeutic inhibition of GM-CSF signalling using monoclonal antibodies to the  $\alpha$ -subunit of the GM-CSF receptor (GMCSFR $\alpha$ ) has shown clear benefit in patients with RA, giant cell arteritis (GCA) and some efficacy in severe SARS-CoV-2 infection. However, GM-CSF autoantibodies are associated with the development of pulmonary alveolar proteinosis (PAP), a rare lung disease characterised by alveolar macrophage (AM) dysfunction and the accumulation of surfactant lipids. We assessed how the anti-GMCSFR $\alpha$  approach might impact surfactant turnover in the airway. Female C57BL/6J mice received a mouse-GMCSFR $\alpha$  blocking antibody (CAM-3003) twice per week for up to 24 weeks. A parallel, comparator cohort of the mouse PAP model, GMCSFR $\beta$  knock-out (KO), was maintained up to 16 weeks. We assessed lung tissue histopathology alongside lung phosphatidylcholine (PC) metabolism using stable isotope lipidomics. GMCSFR $\beta$  KO mice reproduced the histopathological and biochemical features of PAP, accumulating surfactant PC in both broncho-alveolar lavage fluid (BALF) and lavaged lung tissue. The incorporation pattern of *methyl*-D<sub>9</sub>-choline showed impaired catabolism and not enhanced synthesis. In contrast, chronic supra-pharmacological CAM-3003 exposure (100mg/kg) over 24 weeks did not elicit a histopathological PAP phenotype despite some changes in lung PC catabolism. Lack of significant impairment of AM catabolic function supports clinical observations that therapeutic antibodies to this pathway have not been associated with PAP in clinical trials.

## Abbreviations

AM (alveolar macrophage)

BALF (broncho-alveolar lavage fluid)

BMDM (bone marrow derived macrophages)

GM-CSF (granulocyte macrophage colony stimulating factor)

GMCSFR $\alpha$  (GM-CSF receptor alpha subunit)

GMCSFR $\beta$  (GM-CSF receptor beta subunit)

IL (interleukin)

KO (knock-out i.e. of a gene)

MS (mass spectroscopy)

PAP (pulmonary alveolar proteinosis)

PAS (periodic acid-Schiff)

PBS (phosphate buffered saline)

PC (phosphatidylcholine)

RA (rheumatoid arthritis)

SC (subcutaneous)

## Introduction

GM-CSF is a pleiotropic cytokine secreted by immunologically active cells such as T-cells, macrophages and mast cells, as well as structural cells including fibroblasts and endothelial cells (1). Its cognate receptor (GMCSFR) complex is a heterodimer (2) consisting of the GMCSFR $\alpha$  subunit, which confers specificity of GM-CSF signalling, and the GMCSFR $\beta$  chain which is also a component of the interleukin (IL)-3 and IL-5 receptor complexes. GM-CSF has been shown to be involved in multiple biological events (1) and deficiency in GM-CSF signalling in alveolar macrophages is a recognised prelude to PAP, a rare but debilitating human lung disease characterised by accumulation of surfactant proteolipids in the distal airways (3).

In mouse models, genetic ablation of the GM-CSF ligand (4) or of its receptor subunit GMCSFR $\beta$  (5) recapitulates the distinctive lung pathology of surfactant accumulation in the alveolus and BALF (6) of patients with PAP. Although extremely rare, familial forms of PAP have also been identified in man, arising from a loss of function mutation (7) or deletion (8) of GMCSFR $\alpha$ . However, the cause of PAP in most clinical cases is GM-CSF autoimmunity associated with presence of circulating anti-GM-CSF antibodies (9). Underscoring the role of autoimmunity in this disease, experimental clinical studies using either high doses of exogenous recombinant GM-CSF to saturate these antibodies (10) or B-cell depletion using the anti-CD20 antibody rituximab (9), have had some success in restoring normal lung function.

Notwithstanding lung-specific roles and the recognised contribution of GM-CSF to granulocyte haematopoiesis and survival, altered expression of the pathway has been implicated in many inflammatory conditions (1). These include synovial membranes, where GM-CSF is significantly elevated in the synovial fluid of patients with RA (11). GMCSFR $\alpha$  is also up regulated in synovial tissue and on circulating mononuclear cells from RA subjects (12). This knowledge has led to the clinical development of the GM-CSFR $\alpha$ -targeted ligand blocking mAb, mavrilimumab (CAM-3001), for arthritis and related inflammatory diseases (13, 14). Moreover, the distinct role of GM-CSF (15) and emerging data pointing to mavrilimumab efficacy in the treatment of severe SARS-CoV-2 pneumonia and systemic hyperinflammation (16) as well as the GM-CSF over expression in giant cell arteritis (17, 18) emphasises its potential of targeting the GM-CSF axis as an important anti-inflammatory immunotherapy. Recognition that elevated GM-CSF is a key player in severe cytokine

release syndrome (CRS) (19) affirms the targeted reduction approach. Blockade of GM-CSF by lenzilumab moderates the neuroinflammation and enhances the cytotoxicity of Chimeric Antigen Receptor engineered T cells (CAR-T cell) treatment in an acute lymphoblastic leukemia xenograft mouse model (20).

Of note, whilst clinical efficacy in RA has been clearly demonstrated (14, 21) no evidence of PAP has been reported to date (22). Nevertheless, antibody targeting of the GM-CSF axis as a therapeutic strategy in RA raises the question of whether systemic dosing with monoclonal GMCSFR $\alpha$  antibodies could adversely affect distal tissues and modulate airway surfactant metabolism or even induce the PAP phenotype in patients following chronic administration. In a recent primate toxicology study, mavrilimumab showed only minor changes in lung phenotype with no evidence of PAP (23), indicating that a more detailed understanding of the inhibition of this pathway on alveolar function is warranted.

Although clinical diagnosis of PAP is usually confirmed using biopsy material and chest X-ray examination, analysis of lipids in BALF and tissues by mass spectroscopy (MS)-based lipidomic techniques (24) has proven to be a powerful and sensitive tool to study lung lipid metabolism in disease (25) and offers the scope to detect prodromal changes in lung lipid content *in vivo*. In addition, when combined with deuterated lipid precursor incorporation methods (26), they can be used to reveal the contributions of synthesis and catabolism to lipid accumulation *in vivo* (25, 27), and provide detailed quantitative and qualitative characterisation of the lipid molecular species present.

In this study we report the detailed use of lipidomic profiling of phosphatidylcholine (PC) in a mouse model of chronic exposure to a murine GMCSFR $\alpha$  neutralising antibody (CAM-3003) in parallel with a study of the temporal development of lung pathology in the GMCSFR $\beta$  KO mouse.

## **Methods**

### CAM-3003 dosing and *in vivo* procedures

CAM-3003 is a blocking anti mouse GMCSFR $\alpha$  targeting monoclonal mouse IgG1 antibody previously shown to inhibit collagen induced arthritis in DBA/1 mice (12). The potency of this antibody against mouse GM-CSF *in vitro* was confirmed using mouse bone marrow derived macrophages (BMDM). BMDM were pre-incubated with various concentrations (10/1.7/0.28/0.046 nM) of CAM-3003 or an inactive isotype antibody control for 30 min

before being stimulated with 10pg/mL recombinant mouse GM-CSF (R&D Systems, UK) or control for 4h, followed by 100ng/mL LPS (*Salmonella minnesota* R595, Calbiochem) overnight at 37°C. Supernatant IL-6 was measured using an ELISA assay (DY406 from R&D Systems, UK).

All the in vivo work reported here was conducted by Labcorp Drug Development Ltd (formerly Covance Ltd), Harrogate, UK, in an AAALAC accredited facility, after Animal Welfare and Ethical Review Body approval and in adherence with applicable animal welfare regulations. Adult female C57BL/6J mice (Charles River UK Ltd) housed with access *ad libitum* food and water and a 12h light/dark cycle, were dosed with CAM-3003 by SC injection at 0 (vehicle - 50mM sodium acetate, 100mM sodium chloride, pH5.5), 5 or 100mg/kg at twice weekly intervals for up to 24 weeks. The dose volume was 5mL/kg. Animals were allocated to endpoint groups at the start of the study as summarised (Supplementary Table 1). Doses were selected based on previous pharmacodynamic studies to provide a systemic exposure equivalent to therapeutic (5 mg/kg) and supra-therapeutic (100mg/kg) doses. As this study was primarily designed to identify the dose related biological effects of GMCSFR $\alpha$  inhibition, mAb isotype control groups were not included as these would have required significant numbers of additional animals at all dose levels. Female GMCSFR $\beta$  KO mice (B6.129S1-Csf2rb<sup>tm1Cgb</sup>/J) and age and strain matched controls were obtained (The Jackson Laboratory, USA) and maintained at the same facility under the conditions described above. Animals assigned to the 6 week necropsy were approximately 5 weeks old on arrival and were acclimatised for approximately 1 week prior to terminal investigations. Animals assigned to the 12 week necropsy were approximately 10 weeks old on arrival and were acclimatised for approximately 2 weeks prior to terminal investigations. Animals assigned to the 16 week necropsy were approximately 11 weeks old on arrival and were acclimatised for approximately 5 weeks prior to terminal investigations. This strain has previously been shown to be unresponsive to GM-CSF (28). At predetermined time-points throughout the study, selected groups of animals were terminally anaesthetised using isoflurane and a blood sample obtained prior to euthanasia by exsanguination. Lungs were removed and weighed before fixation or snap freezing. For sub-groups of animals, lung PC synthesis was assessed by intraperitoneal injection of 0.1 mg deuterated choline (*methyl-D<sub>9</sub>*-choline chloride, CK Gas Products UK) at 5, 10, 24 or 48h before terminal sampling as described previously (29). BALF samples were collected using 4 x 1mL volumes of PBS, and plasma and BALF supernatant aliquots stored at <-50°C. Additional parallel groups of

animals were used to assess pharmacokinetic parameters. Serum CAM-3003 levels were quantified using a sandwich immunoassay method on the Gyrolab platform. CAM-3003 in standards, controls and samples was captured by a biotinylated murine GM-CSFR alpha at 100µg/mL (R&D Systems, UK) and detected by an Alexa-labelled rabbit anti-mouse IgG4 Affinity Purified PAb antibody at 30nM (Invitrogen, UK) on a Gyrolab Bioaffy 200 CD platform (Gyros AB, Sweden). Analysis was performed using the Gyrolab Evaluator software using a 5-parameter logistical curve fit with a  $1/y^2$  weighting factor.

To confirm the immune-reactive CAM-3003 retained functional GMCSF antagonism during the study, the GM-CSF blocking activity of serum was determined at day 108 (week 15) in a subset of serum samples using mouse bone marrow derived macrophages (BMDM). BMDM were pre-incubated with 10nM of CAM-3003, 10nM of an inactive isotype antibody control or serum from dosed mice diluted to a final concentration of 10nM of CAM-3003 for 30 min before being stimulated with 10pg/ml recombinant mouse GM-CSF (R&D Systems) or control overnight at 37°C. Supernatant TARC was measured using an ELISA assay (DY529 from R&D, UK), to demonstrate pharmacological suppression of GM-CSF signalling.

### **Histological assessment**

Post-mortem lung tissue samples were formalin fixed and paraffin embedded, 5µm sectioned and stained with haematoxylin and eosin, and PAS methods to reveal structural and pathophysiological features. Slides were assessed by a pathologist blinded to treatment.

### **Lung phospholipid analyses**

BALF and lung tissue homogenates in PBS were extracted, in batches of 24, on a robotic liquid handling platform using a Bligh & Dyer methodology (30) modified, after experimental validation in house, to use dichloromethane instead of chloroform. The prior addition of a phospholipid internal standards mix as described previously (31) permitted quantitation of major phospholipid classes as well as individual molecular species. Butylated hydroxytoluene (BHT, 0.01%) was used throughout extractions to minimise oxidation and total lipid extracts were stored under nitrogen at -80°C prior to mass spectrometry. All lipidomic analyses, including calculations of absolute rates of lung tissue PC synthesis, were undertaken as described elsewhere (27) except that mass spectrometry was undertaken by direct infusion of lipid extracts using a XEVO TQ mass spectrometer (Waters, Milford Massachusetts).

## Statistics

Unless otherwise stated, all statistical tests were undertaken using GraphPad Prism v8 software.

## Results

Before starting the 24-week chronic study, bioactivity of the batch of CAM-3003 antibody that was to be used throughout was confirmed. Incubation of mouse BMDMs with GM-CSF and LPS induces the release of the proinflammatory cytokine IL-6 into the culture supernatant (Figure 1). Pre-incubation with CAM-3003, but not isotype control antibody, to the BMDMs elicits a concentration dependent inhibition of IL-6 release with sub-nanomolar potency (IC<sub>50</sub> ~10pM).

Wild-type C57BL/6J mice received twice weekly SC injection with either vehicle alone or CAM-3003 at 5mg/kg or 100mg/kg. A separate cohort of satellite animals, which were not analysed for histology, also received CAM-3003 at these doses and were culled at approximately monthly intervals up to day 165 (week 24) of the experiment. Serum was assayed for CAM-3003 concentration using an ELISA and as shown in Figure 2A, these doses resulted in peak serum exposures of ~100µg/mL and ~1000µg/mL respectively for 5 months with no evidence of anti-drug antibody induced clearance observed. The pharmacological activity of the serum CAM-3003 during the later phase of the study was confirmed using *in vitro* cytokine release assays (Figure 2B). Serum samples from day 109 (week 16) endpoints showed marked inhibition of TARC in a GM-CSF dependent assay, indirectly demonstrating the blocking activity of these antibodies throughout the study.

Animal bodyweight and terminal lung wet weights were measured in the CAM-3003 or vehicle dosed cohort as well as in the GMCSFRβ KO mice. GMCSFRβ KO mice lung wet weight, but not bodyweight, continued to increase at 12 and 16 weeks of age compared to the WT control mice, whilst animals receiving CAM-3003 at 5mg/kg or 100mg/kg showed no increase in lung wet weight or body weight relative to vehicle dosed animals (Supplementary Figure 1). CAM-3003 and vehicle dosing was continued out to 24 weeks with no further change in lung or bodyweight (data not shown).

Lung tissues obtained from GMCSFRβ KO mice and their wild-type counterparts at 6, 12 and 16 weeks of age were assessed by a pathologist who was blinded with respect to their genotype (Figure 3A). GMCSFRβ KO mice displayed characteristic features of PAP-like

disease, with alveolar accumulation of PAS-positive material, which increased from 6 to 16 weeks of age. Aged matched wild-type mice showed no alveolar abnormality. Lungs from CAM-3003 and vehicle dosed C57BL/6J mice were assessed in an identical way after dosing for up to 24 weeks (Figure 3B). As reported by the pathologist, there was no evidence of gross changes in the lung tissue or alveolar spaces at any of the time points examined or doses of CAM-3003. At high power macrophages stained positive with eosin were observed in occasional animals from all groups, including controls. The cytoplasm in these macrophages stained positively for PAS (Supplementary Figure 2).

Measurement of the PC content of lavaged lung homogenates showed a threefold increase in the PC recovered from GMCSFR $\beta$  KO animals compared with their WT controls, 48.22 nmoles/100 $\mu$ L  $\pm$  5.20 nmoles/100 $\mu$ L versus 150.79 nmoles/100 $\mu$ L  $\pm$  30.34 nmoles/100 $\mu$ L (means  $\pm$  SD, n=25 in each group). This was consistent with the lung tissue accumulation of surfactant lipid previously seen using this methodology in the GM-CSF ablation PAP mouse phenotype (25).

Total PC was likewise measured in the BALF of GMCSFR $\beta$  KO animals compared with their WT controls at 12 weeks of age (84 days). The GMCSFR $\beta$  KO animals exhibited a clear 3.5-fold increase in the total PC recovered by lavage, 443.93  $\pm$  65.99 nmoles, compared with the WT controls, 127.02  $\pm$  14.99 nmoles PC (mean  $\pm$  SD, n = 25 in each group, p<0.0001). Analysis of the BALF of CAM-3003 dosed WT animals after 24 weeks of exposure (Figure 4) showed that the concentration of PC in the CAM-3003 treated and vehicle control animals was unchanged,

A detailed comparison of lavaged lung tissue PC and the BALF PC composition from the same lungs was also carried out to characterise the changes in specific molecular species, particularly those which are the main components of pulmonary surfactant such as PC16:0/16:0 and PC16:0/16:1. The actual composition of PC in BALF was unaltered across all groups with respect to the proportions of lipid species present (Figure 5A). Mice which had received vehicle or CAM-3003 at either dose for 24 weeks had equivalent proportions of lipid species in BALF which were not different to the GMCSFR $\beta$  KO mice or their wild-type controls at 16 weeks of age.

In homogenates of the lavaged lungs obtained from the GMCSFR $\beta$  KO mice the magnitude of increase in the proportions of PC16:0/16:0 (from 29.2%  $\pm$  1.47% rising to 41.17%  $\pm$  1.22%) and PC16:0/16:1 (from 14.79%  $\pm$  1.67% rising to 21.98%  $\pm$  1.36%) relative to the

WT controls consistent with the established phenotype of tissue lipid accumulation in the lungs of PAP mice (25, 28). Coupled with the large number of measurements made ( $n = 25$  mice/group), this selective surfactant lipid species accumulation resulted in every other proportion of PC molecular species differing significantly ( $p < 0.0001$ ) from the control group (Figure 5B). However, there were no significant changes in the PC compositions of lung homogenate obtained from CAM-3003 dosed animals compared to vehicle.

In order to determine the synthetic and catabolic rates of PC turnover, deuterated *methyl-D<sub>9</sub>*-choline was administered, via intraperitoneal injection, into CAM-3003 dosed mice, in weeks 16 (113 days) and 24 (169 days), or GMCSFR $\beta$  KO mice and WT controls at 12 weeks of age (84 days). Enrichment into both lung tissue and corresponding BALF samples was followed for 48h. Detectable incorporation of the stable isotope into PC species was evident in lavaged lungs and BALF at each sampled time point (Figure 6). The enrichment of the lavaged lung homogenate total PC pool by these deuterated species over 48h showed that between 0 and 6 h the proportion of total lung tissue PC containing *methyl-D<sub>9</sub>*-choline had increased to greater than 1.5% in the vehicle, 5mg/kg and 100mg/kg treated mice (Figure 6A, 6B).

Vehicle control mice showed comparable incorporation of *methyl-D<sub>9</sub>*-choline into the lavaged lung tissue PC pool indicating that CAM-3003-treated mice behave essentially identically (Figure 6C). In the GMCSFR $\beta$  KO mice with an accumulated surfactant PC pool within their lavaged lung tissues, however, the proportion of lung PC with *methyl-D<sub>9</sub>*-choline remained less than 0.5% (Figure 6C).

BALF from the same mice was analysed for *methyl-D<sub>9</sub>*-choline enrichment (Figure 6 D-F). GMCSFR $\beta$  KO mice (Figure 6F) showed a reduced enrichment of *methyl-D<sub>9</sub>*-choline compared to their age-matched wild-type controls at every time point, which is consistent with dilution of newly synthesised and secreted surfactant PC into the higher total PC content of BALF as shown in Figure 4 and supplementary Table 2. In contrast to the tissue PC enrichment, the *methyl-D<sub>9</sub>*-choline enrichment in the surfactant PC of BALF at both 10h and 24h from animals dosed with 5mg/kg CAM-3003 for 16 weeks (Figure 6D) or 100mg/kg CAM-3003 for 24 weeks (Figure 6E) showed a significantly different profile to vehicle dosed animals ( $p < 0.05$  for 16 week animals and  $p < 0.005$  for 24 week animals at each dose). The rate of appearance of *methyl-D<sub>9</sub>*-choline containing PC appears lower for CAM-3003 dosed

animals compared to vehicle, with peak enrichment at 24 hours of 1.25% for mAb treated animals compared to 1.75% for vehicle controls.

The ratio of *methyl-D<sub>9</sub>*-choline enrichment in BALF and lung tissue (Figure 7) is independent of any variation in substrate labelling. It clearly demonstrates that, while trends but no statistically significant differences are apparent in the week 16 data (Figure 7A), both secretion and catabolism are decreased in the 100mg/kg CAM-3003 dose group at week 24 (Figure 7B). The low values for GMCSFR $\beta$  KO mice compared to WT controls (Figure 7C) are due to secretion into a much larger PC pool.

Together these static and dynamic lipidomic data show that prolonged exposure (24 weeks) to a supra-pharmacological dose of CAM-3003 at 100mg/kg results in a slowing of newly synthesised lung surfactant PC secretion into the alveolar space and to its subsequent turnover. However, this is not accompanied with a PAP phenotype suggesting that such variation is accommodated by normal homeostasis mechanisms which operate to maintain equilibrium.

## **Discussion**

The pleiotropic cytokine GM-CSF has multiple biological properties including involvement in chronic tissue inflammation scenarios such as RA (11, 12), where unbalanced, excess GMCSFR signalling is apparent. Elevated GM-CSF in RA synovial fluid (32) along with an upregulation of GMCSFR $\alpha$  in synovial tissues and circulating monocytes (12) contributes to the pathology by stimulating the proliferation and differentiation of myeloid lineage inflammatory cells from bone marrow progenitors (33). However, genetic ablation of normal GMCSFR signalling via GM-CSF results in a disruption in AM function (34) leading to alveolar accumulations of the lipoproteinaceous material characteristic of PAP.

Blockade of the GMCSFR has proven to be a successful therapeutic strategy, attenuating aberrant GM-CSF signalling in patients with RA (35). Indeed, the pharmacological targeting of GMCSFR $\alpha$  with the monoclonal antibody Mavrimumab (CAM-3001) in human RA patients has shown significant reductions in disease activity (14). More recently emerging data suggests that the same strategy may be effective in patients with severe SARS-CoV-2 infection (15, 16) where GM-CSF has been shown to have a key role (15). Most clinical cases of PAP arise from GM-CSF autoantibodies, an anti-ligand phenomenon, rather than by blocking GMCSFR engagement. Importantly, it appears that multiple polyclonal antibodies

are needed to inhibit GM-CSF bioactivity and block function (36). The *in vivo* binding of up to two different, patient derived anti-GM-CSF mAbs could result in the persistence of hGM-CSF in serum of injected mice (ie by extending the circulating half-life), whereas binding of hGM-CSF by three non-overlapping antibodies leads to the rapid clearance of circulating ligand-antibody complexes (36). This process appears to be Fc $\gamma$ -R dependent and GM-CSF suppression by sequestration and depletion of ligand is different to the functional antagonism of an anti-receptor monoclonal antibody, which may be one explanation for the lack of lung pathology seen in the clinic (14, 22).

While no evidence of PAP from mavrilimumab (CAM-3001) treated patients has been reported to date, our observations now provide important insights to the robustness of homeostatic mechanisms in the murine model of arthritis dosed with CAM-3003, the efficacious, surrogate mouse mAb for mavrilimumab (12). These may also inform human use of CAM-3001 explaining the lack of currently observed deleterious effects of the antibody therapy upon lung lipid metabolism.

Our validation of the experimental model of chronic CAM-3003 dosing of mice for up to six months confirmed the blockade of GM-CSF signalling *in vitro* (Supplementary Figure 1), sustained serum concentrations of antibody (Figure 2A) and blockade of GM-CSF responses *ex vivo* (Figure 2B). Accordingly, we were able to use the model for evaluation of any lung-specific consequences of chronic GMCSFR blockade. In parallel investigations, cohorts of GMCSFR $\beta$  KO mice maintained up to 16 weeks of age, provided a necessary reference model for the biochemical and pathological features of the PAP-like phenotype as they develop.

Throughout these studies the only group where lung wet weight continued to increase (Supplementary Figure 2) were the GMCSFR $\beta$  KO mice. This was likely due to accumulating lipoprotein in the lung lumen. By 16 weeks of age they had clearly recognisable PAP-like features; alveolar accumulation of PAS-positive staining material and lipid in the surrounding tissue (Figure 3A) characteristic of surfactant accretion. In contrast, the CAM-3003 dosed animals, despite having supra-pharmacological levels of antibody in circulation, showed no evidence of excess surfactant material (Figure 3B).

Lack of a PAP-like phenotype in the CAM-3003 treated animals could not preclude a shift in the equilibrium of lung PC turnover while remaining within the normal, homeostasis range. Accordingly, in order to probe further into the consequences of GM-CSF blockade on lung

lipid metabolism and catabolism, mass spectrometry was used to measure total PC in lavaged lung tissue and BALF. This method has previously revealed the impact on phospholipids in other surfactant disorders in animal and human studies (25, 27, 37).

Total PC was only increased in the BALF and lavaged lung tissue from GMCSFR $\beta$  KO mice (Figure 4) with molecular species patterns confirming the accumulation of surfactant PC seen in the histology. This reflects a clear perturbation of the tissue steady-state PC homeostasis that is manifest as PAP over time. The threefold increase in the observed tissue PC content after 12 weeks was accompanied by proportional representations of specific PC molecular species, PC16:0/16:0 and PC16:0/16:1, major components of surfactant. Increased intracellular surfactant accumulation is also a PAP characteristic.

These data were consistent with the PAP previously seen in both the GM-CSF ablation and GMCSFR $\beta$  KO mouse models (4, 6, 25). In contrast, there was no histological or PC content evidence of PAP after twenty-four weeks of WT mouse CAM-3003 exposure. Indeed, it did not appear to have any impact on BALF total PC, nor on its molecular species composition (Figure 5A).

The principal mechanistic consequence of AM compromise seen in PAP lies in inadequate surfactant clearance and catabolism (34). Consequently, to confirm a mismatch in PC catabolism versus synthesis in relation to the observed increase in BALF PC in the GMCSFR $\beta$  KO mice, incorporation of *methyl-D<sub>9</sub>*-choline was used to track the appearance of newly formed PC species in lung tissue (Figure 6C) and BALF (Figure 6F). Airway alveolar type-II cells continuously synthesise new surfactant phospholipids for incorporation into lamellar bodies and later release into the airway lumen to maintain a reduced airway surface tension that facilitates gas exchange (27). The deuterated choline is taken up in these cells and incorporated into newly synthesised PC. Monitoring the appearance of *methyl-D<sub>9</sub>*-choline containing PC species in the BALF and tissue provides a highly accurate readout of PC synthesis *in vivo* (27).

In the GMCSFR $\beta$  KO mice, the enrichment of lavaged lung tissue PC with newly synthesised *methyl-D<sub>9</sub>*-choline containing surfactant PC species over the 48-hour labelling time course was lower (Figure 6C) than in the aged matched controls due to dilution in the larger PC pool. The corresponding BALF PC measurements also demonstrated greater dilution of *methyl-D<sub>9</sub>*-choline label in the larger pool from the KO animals (Figure 6B).

When the figures are examined as BALF/Lung tissue ratio (Figure 7C) the dilution effect is even more apparent.

In contrast, there were no differences in the lavaged lung tissue PC enrichment with *methyl-D<sub>9</sub>*-choline containing species between the CAM-3003 dosed and vehicle animals, consistent with the similar pool sizes of their tissue PC. The 48h time-course data also indicated that CAM-3003 exposure does not alter the synthesis of *methyl-D<sub>9</sub>* containing surfactant PC molecular species in alveolar type-II cells. However, time-course data did show a delayed appearance of *methyl-D<sub>9</sub>*-choline PC in the BALF of CAM-3003 dosed animals which reached parity with that of the control animals by 48h. This observation was seen in the supra-pharmacological dose (100mg/kg CAM-3003) and to a lesser extent at the lower, therapeutic equivalent (5mg/Kg) dose when the data was presented as BALF/lung tissue ratio (Figures 7A & 7B) indicating that it is independent of any inter-animal variation in intracellular *methyl-D<sub>9</sub>*-choline labelling. A normal equilibrium position was reached by 48h and it seems clear that, rather than being without effect, there is a disturbance in surfactant PC secretion/turnover, albeit one that is accommodated within normal homeostasis mechanisms even at supra-pharmacological doses of CAM-3003. In the absence of isotype control mAb dosed groups we cannot preclude a non-specific effect although given the sensitivity of our analytical methods we consider this unlikely. Importantly, it should be noted that the extent to which homeostasis mechanisms are able to maintain surfactant turnover equilibrium could potentially be overwhelmed in patients with an already compromised surfactant metabolism. There may therefore be a rationale for regular monitoring of the lungs of patients with such comorbidities alongside therapeutic targeting of the GM-CSF axis.

In summary, knowing that most clinical cases of PAP are due to autoantibodies to GM-CSF and that use of Mavrimumab in RA has not been linked with human PAP, we sought to understand the effects of a monoclonal GMCSFR $\alpha$  antibody on the mouse lung, and to understand at a biochemical level the impact of such pharmacological and supra-pharmacological dosing on airway surfactant homeostasis. The clear PAP-like pathology seen in GMCSFR $\beta$  KO model mice was not recapitulated by chronic exposure to supra-pharmacological levels of a potent GMCSFR $\alpha$  mAb, either in airway structure or PC content. We did, however, observe some changes in appearance of newly synthesised PC content of BALF in mice with very high (>1mg/ml) serum exposures to CAM-3003. This was

particularly intriguing, as no change in lung tissue incorporation was seen, but appears to lie within the range where homeostasis mechanisms are able to maintain normal function.

### **Clinical Perspectives**

- GM-CSF autoantibodies generally result in PAP, yet clinical use of the GMCSFR $\alpha$  mAb, Mavrilimumab, in RA has not currently been shown to evoke PAP.
- Chronic exposure of C57BL/6J mice to supra-pharmacological doses of the equivalent murine GMCSFR $\alpha$  mAb, CAM-3003, disturbs surfactant PC turnover without recapitulating the PAP-like pathology seen in GMCSFR $\beta$  KO mice.
- Despite altered surfactant turnover, homeostatic mechanisms are sufficient to explain the absence of PAP in individuals treated with GMCSFR $\alpha$  mAb for RA, severe SARS-CoV-2 infection or other inflammatory over-expressions of GM-CSF.

### **Data availability**

Curated data mass spectrometry data and any other relevant data will be supplied by the corresponding authors upon reasonable request.

### **Acknowledgements**

Alison Dodd.

### **Source of Funding**

This work was funded by MedImmune/Astrazeneca.

### **Conflicts of interest**

Authors who are listed as AstraZeneca employees may have held stock/stock options in AstraZeneca Plc at the time this work was carried out.

### **References**

1. Becher B, Tugues S, Greter M. GM-CSF: From Growth Factor to Central Mediator of Tissue Inflammation. *Immunity*. 2016;45(5):963-73.
2. Cook AD, Hamilton JA. Investigational therapies targeting the granulocyte macrophage colony-stimulating factor receptor-alpha in rheumatoid arthritis: focus on mavrilimumab. *Ther Adv Musculoskelet Dis*. 2018;10(2):29-38.
3. Suzuki T, Trapnell BC. Pulmonary Alveolar Proteinosis Syndrome. *Clin Chest Med*. 2016;37(3):431-40.

4. Dranoff G, Crawford AD, Sadelain M, Ream B, Rashid A, Bronson RT, et al. Involvement of granulocyte-macrophage colony-stimulating factor in pulmonary homeostasis. *Science*. 1994;264(5159):713-6.
5. Nishinakamura R, Nakayama N, Hirabayashi Y, Inoue T, Aud D, McNeil T, et al. Mice deficient for the IL-3/GM-CSF/IL-5 beta c receptor exhibit lung pathology and impaired immune response, while beta IL3 receptor-deficient mice are normal. *Immunity*. 1995;2(3):211-22.
6. Ikegami M, Ueda T, Hull W, Whitsett JA, Mulligan RC, Dranoff G, et al. Surfactant metabolism in transgenic mice after granulocyte macrophage-colony stimulating factor ablation. *Am J Physiol*. 1996;270(4 Pt 1):L650-8.
7. Suzuki T, Sakagami T, Rubin BK, Nogee LM, Wood RE, Zimmerman SL, et al. Familial pulmonary alveolar proteinosis caused by mutations in CSF2RA. *J Exp Med*. 2008;205(12):2703-10.
8. Martinez-Moczygomba M, Doan ML, Elidemir O, Fan LL, Cheung SW, Lei JT, et al. Pulmonary alveolar proteinosis caused by deletion of the GM-CSFRalpha gene in the X chromosome pseudoautosomal region 1. *J Exp Med*. 2008;205(12):2711-6.
9. Thomassen MJ, Yi T, Raychaudhuri B, Malur A, Kavuru MS. Pulmonary alveolar proteinosis is a disease of decreased availability of GM-CSF rather than an intrinsic cellular defect. *Clin Immunol*. 2000;95(2):85-92.
10. Tazawa R, Trapnell BC, Inoue Y, Arai T, Takada T, Nasuhara Y, et al. Inhaled granulocyte/macrophage-colony stimulating factor as therapy for pulmonary alveolar proteinosis. *Am J Respir Crit Care Med*. 2010;181(12):1345-54.
11. Williamson DJ, Begley CG, Vadas MA, Metcalf D. The detection and initial characterization of colony-stimulating factors in synovial fluid. *Clin Exp Immunol*. 1988;72(1):67-73.
12. Greven DE, Cohen ES, Gerlag DM, Campbell J, Woods J, Davis N, et al. Preclinical characterisation of the GM-CSF receptor as a therapeutic target in rheumatoid arthritis. *Ann Rheum Dis*. 2015;74(10):1924-30.
13. van Nieuwenhuijze A, Koenders M, Roeleveld D, Sleeman MA, van den Berg W, Wicks IP. GM-CSF as a therapeutic target in inflammatory diseases. *Mol Immunol*. 2013;56(4):675-82.
14. Burmester GR, McInnes IB, Kremer J, Miranda P, Korkosz M, Vencovsky J, et al. A randomised phase IIb study of mavrilimumab, a novel GM-CSF receptor alpha monoclonal antibody, in the treatment of rheumatoid arthritis. *Ann Rheum Dis*. 2017;76(6):1020-30.
15. Thwaites RS, Sanchez Sevilla Uruchurtu A, Siggins MK, Liew F, Russell CD, Moore SC, et al. Inflammatory profiles across the spectrum of disease reveal a distinct role for GM-CSF in severe COVID-19. *Sci Immunol*. 2021;6(57).
16. De Luca G, Cavalli G, Campochiaro C, Della-Torre E, Angelillo P, Tomelleri A, et al. GM-CSF blockade with mavrilimumab in severe COVID-19 pneumonia and systemic hyperinflammation: a single-centre, prospective cohort study. *Lancet Rheumatol*. 2020;2(8):e465-e73.
17. Cid MC, Gandhi R, Corbera-Bellalta M, Muralidharan S, Paolini JF. Gm-Csf Pathway Signature Identified in Temporal Artery Biopsies of Patients with Giant Cell Arteritis. *Annals of the Rheumatic Diseases*. 2019;78:271-2.
18. Cid MC, Muralidharan S, Corbera-Bellalta M, Espigol-Frigole G, Marco Hernandez J, Denuc A, et al. FRI0010 GM-CSFR PATHWAY IS IMPLICATED IN PATHOGENIC INFLAMMATORY MECHANISMS IN GIANT CELL ARTERITIS. *Annals of the Rheumatic Diseases*. 2020;79(Suppl 1):576-.
19. Morris EC, Neelapu SS, Giavridis T, Sadelain M. Cytokine release syndrome and associated neurotoxicity in cancer immunotherapy. *Nat Rev Immunol*. 2021.
20. Sterner RM, Sakemura R, Cox MJ, Yang N, Khadka RH, Forsman CL, et al. GM-CSF inhibition reduces cytokine release syndrome and neuroinflammation but enhances CAR-T cell function in xenografts. *Blood*. 2019;133(7):697-709.
21. Weinblatt ME, McInnes IB, Kremer JM, Miranda P, Vencovsky J, Guo X, et al. A Randomized Phase IIb Study of Mavrilimumab and Golimumab in Rheumatoid Arthritis. *Arthritis Rheumatol*. 2018;70(1):49-59.

22. Burmester GR, McInnes IB, Kremer JM, Miranda P, Vencovsky J, Godwood A, et al. Mavrilimumab, a Fully Human Granulocyte-Macrophage Colony-Stimulating Factor Receptor alpha Monoclonal Antibody: Long-Term Safety and Efficacy in Patients With Rheumatoid Arthritis. *Arthritis Rheumatol*. 2018;70(5):679-89.
23. Ryan PC, Sleeman MA, Rebelatto M, Wang B, Lu H, Chen X, et al. Nonclinical safety of mavrilimumab, an anti-GM-CSF receptor alpha monoclonal antibody, in cynomolgus monkeys: relevance for human safety. *Toxicol Appl Pharmacol*. 2014;279(2):230-9.
24. Postle AD, Wilton DC, Hunt AN, Attard GS. Probing phospholipid dynamics by electrospray ionisation mass spectrometry. *Prog Lipid Res*. 2007;46(3-4):200-24.
25. Hunt AN, Malur A, Monfort T, Lagoudakis P, Mahajan S, Postle AD, et al. Hepatic Steatosis Accompanies Pulmonary Alveolar Proteinosis. *Am J Respir Cell Mol Biol*. 2017;57(4):448-58.
26. Postle AD, Hunt AN. Dynamic lipidomics with stable isotope labelling. *J Chromatogr B Analyt Technol Biomed Life Sci*. 2009;877(26):2716-21.
27. Postle AD, Henderson NG, Koster G, Clark HW, Hunt AN. Analysis of lung surfactant phosphatidylcholine metabolism in transgenic mice using stable isotopes. *Chem Phys Lipids*. 2011;164(6):549-55.
28. Robb L, Drinkwater CC, Metcalf D, Li R, Kontgen F, Nicola NA, et al. Hematopoietic and lung abnormalities in mice with a null mutation of the common beta subunit of the receptors for granulocyte-macrophage colony-stimulating factor and interleukins 3 and 5. *Proc Natl Acad Sci U S A*. 1995;92(21):9565-9.
29. Pynn CJ, Henderson NG, Clark H, Koster G, Bernhard W, Postle AD. Specificity and rate of human and mouse liver and plasma phosphatidylcholine synthesis analyzed in vivo. *J Lipid Res*. 2011;52(2):399-407.
30. Bligh EG, Dyer WJ. A rapid method of total lipid extraction and purification. *Can J Biochem Physiol*. 1959;37(8):911-7.
31. Hunt AN, Clark GT, Attard GS, Postle AD. Highly saturated endonuclear phosphatidylcholine is synthesized in situ and colocalized with CDP-choline pathway enzymes. *J Biol Chem*. 2001;276(11):8492-9.
32. Bell AL, Magill MK, McKane WR, Kirk F, Irvine AE. Measurement of colony-stimulating factors in synovial fluid: potential clinical value. *Rheumatol Int*. 1995;14(5):177-82.
33. Hamilton JA. GM-CSF in inflammation. *J Exp Med*. 2020;217(1).
34. Trapnell BC, Nakata K, Bonella F, Campo I, Griese M, Hamilton J, et al. Pulmonary alveolar proteinosis. *Nat Rev Dis Primers*. 2019;5(1):16.
35. Avci AB, Feist E, Burmester GR. Targeting GM-CSF in rheumatoid arthritis. *Clin Exp Rheumatol*. 2016;34(4 Suppl 98):39-44.
36. Piccoli L, Campo I, Fregni CS, Rodriguez BM, Minola A, Sallusto F, et al. Neutralization and clearance of GM-CSF by autoantibodies in pulmonary alveolar proteinosis. *Nat Commun*. 2015;6:7375.
37. Brandsma J, Goss VM, Yang X, Bakke PS, Caruso M, Chanez P, et al. Lipid phenotyping of lung epithelial lining fluid in healthy human volunteers. *Metabolomics*. 2018;14(10):123.

## Figure Legends

### **Figure 1: CAM-3003 inhibits GM-CSF potentiation of LPS induced IL-6 production in mouse BMDM**

Mouse BMDM were pre-incubated with a titration of anti-GM-CSFR $\alpha$  mAb, CAM-3003, or an irrelevant isotype mAb control prior to being primed with 10pg/ml GM-CSF or not for

4hrs followed by overnight stimulation with or without 10ng/ml LPS. IL-6 levels in the supernatant were determined. All measurements were duplicates and data shown are mean  $\pm$  SD of 2 animals. Unpaired t-test comparing measured IL-6 content between CAM-3003 and isotype control treated cells at the same concentration (\*  $p < 0.05$ , n.s. – not significant).

**Figure 2A : Pharmacokinetic profile of CAM-3003 measure in mouse serum up to 24 weeks.**

Mouse serum concentrations of CAM-3003 were quantified using a Gyrolab Workstation (Gyros) using recombinant mouse GMCSFR $\alpha$  capture and rabbit anti-mouse IgG4 detection antibody. Data shown as mean  $\pm$  SD, all points n=3.

**Figure 2B: Serum from CAM-3003 dosed mice at 16 weeks (day 109) potently inhibits TARC production in response to GM-CSF *in vitro***

Mouse BMDM were pre-incubated with 10nM of anti-GM-CSFR $\alpha$ , CAM-3003, an irrelevant isotype control, or serum collected from CAM-3003 dosed mice at day 109 (serum obtained prior to the next dose i.e. at trough); prior to being primed with 10pg/ml GM-CSF followed by overnight stimulation. TARC levels in the supernatant were determined. One-way ANOVA followed by Sidak's multiple comparisons test (GraphPad Prism 9.0.0). (\*\*\*\*  $P < 0.001$ ; \*\*\*  $P < 0.01$ ). All measurements were duplicates and data shown are mean  $\pm$  SEM of 2 animals.

**Figure 3**

Panel A shows representative histopathological images of lungs of GMCSFR $\beta$  mice from 6 to 16 weeks, with characteristic development of PAP-like phenotype. Note the presence of amorphous, eosinophilic and PAS+ material in lumina of alveoli (arrow). Panel B shows representative images from CAM-3003 or vehicle treated animals with no overt pathology.

**Figure 4 BALF PC recovered from CAM-3003 dosed mice compared with GMCSFR $\beta$  KO mice**

Left Panel shows PC concentrations in CAM-3003 dosed animals and their controls for each treatment group (mean  $\pm$  SEM, n = 5. for each group) there were no significant differences

apparent between any dosed animal groups. The right panel shows equivalent measurements for GMCSFR $\beta$  KO mice and their controls (mean  $\pm$  SEM, n = 25 for each group) with a 3.5-fold increase in recovered PC, p<0.0001

**Figure 5. PC molecular species compositions of lavaged lungs and corresponding BALF samples**

(A) Proportional representation of all PC species > 0.5% total PC in BALF from control, CAM-3003 dosed and GMCSFR $\beta$  KO mice (mean  $\pm$  SEM, n = 5 and 25). There are no significant differences in the molecular species compositions of recovered BALF from any groups (B) Proportional representation of all PC species > 0.5% total PC in lavaged lung tissue from the same control, CAM-3003 dosed and GMCSFR $\beta$  KO mice (mean  $\pm$  SEM, n = 5 and 25). Saturated, surfactant-associated PC species are significantly elevated in GMCSFR $\beta$  KO mice, p<0.0001

**Figure 6 Incorporation of *methyl-D9*-choline into the lung and BALF PC of CAM-3003 dosed mice as a proportion of total PC**

Time course determinations over 48 hours of *methyl-D9*-choline headgroup incorporation into the unlabelled PC pool (% Enrichment) for groups of CAM-3003 dosed and GMCSFR $\beta$  KO mice. Panels (A) & (D) Lung and BALF PC enrichments of mice treated for 113 days with pharmacological and supra-pharmacological doses of CAM-3003 and untreated controls (n = 5 in each group). Panels (B) & (E) Lung and BALF PC enrichments of mice treated for 169 days with pharmacological and supra-pharmacological doses of CAM-3003 and untreated controls (n = 5 in each group). Panels (C) & (F) Lung and BALF PC enrichments of GMCSFR $\beta$  KO mice at 84 days and their age-matched controls (n = 5 in each group)

**Figure 7. The ratio of BALF/Lung PC enrichment with *methyl-D9*-choline**

Incorporation of *methyl-D<sub>9</sub>*-choline into PC expressed as a ratio of BALF:lung homogenate enrichments. Panel A shows ratioed 48-hour time course data from CAM-3003 dosed animals and controls at 113 days. Panel B shows ratioed 48-hour time course data from CAM-3003 dosed animals and controls at 169 days. Panel C shows ratioed 48-hour time course data from GMCSFR $\beta$  KO mice at 84 days and their age-matched controls.

Figure 1

**CAM-3003 inhibits GMCSF and LPS induced IL-6 production in mouse bone marrow derived macrophages (BMDM)**

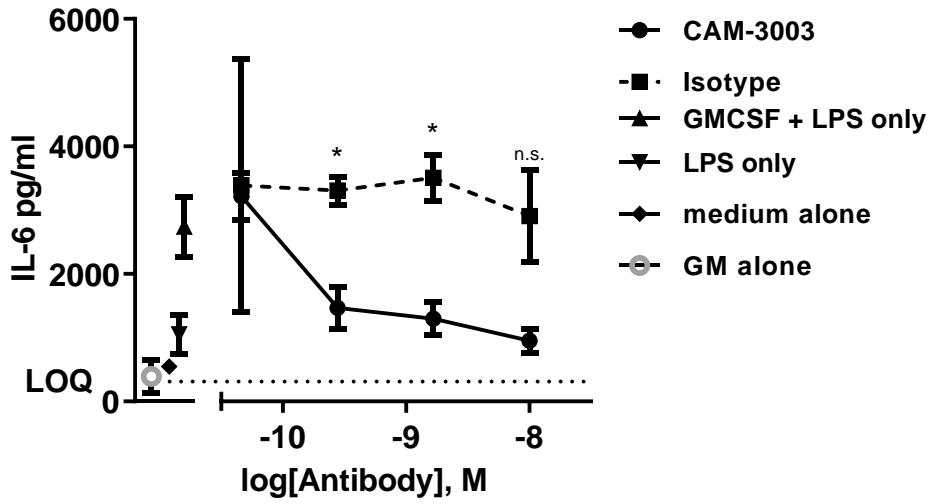


Figure 2A – Serum exposure profile of CAM-3003

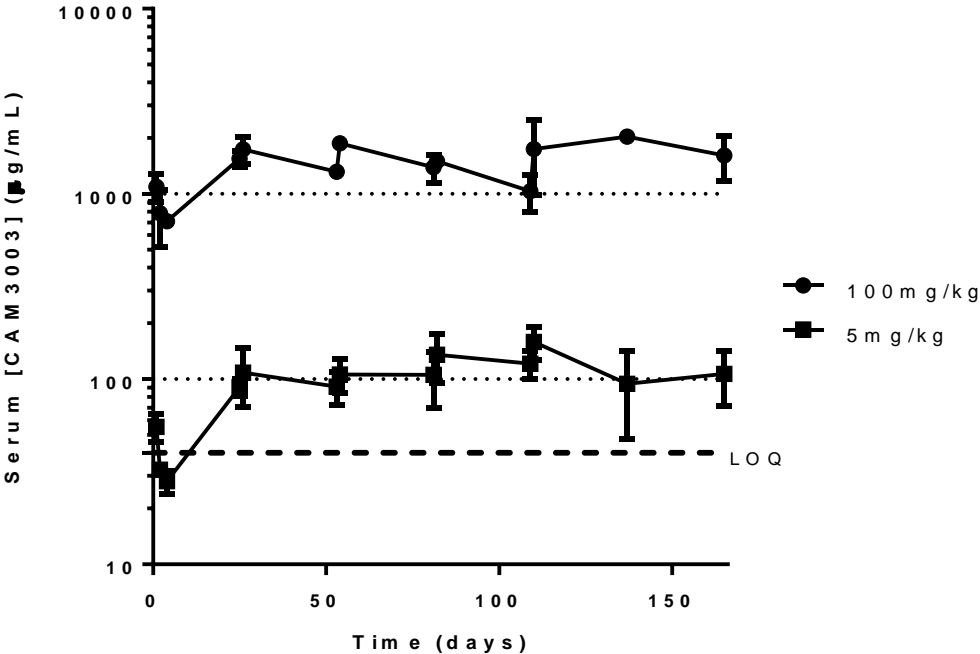


Figure 2B

Serum from CAM-3003 dosed mice at 16 weeks (day 109) potently inhibits responses to GMCSF *in vitro*

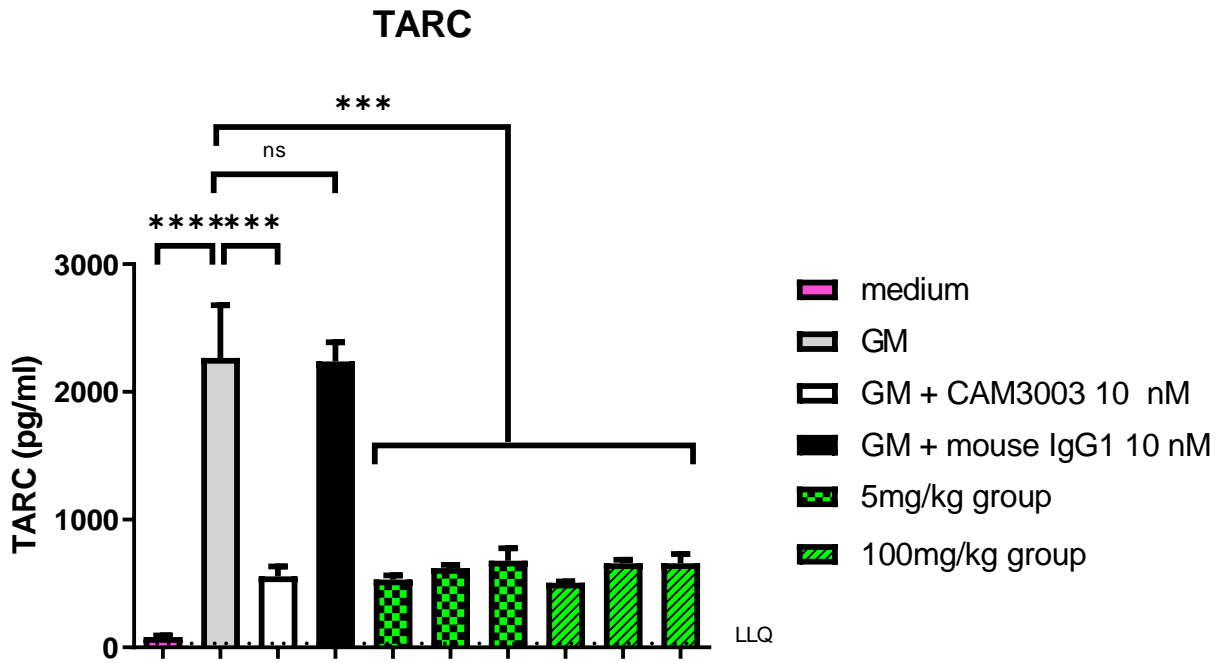


Figure 3A

GMCSFR $\beta$  KO mice lungs show characteristic features of PAP-like disease.

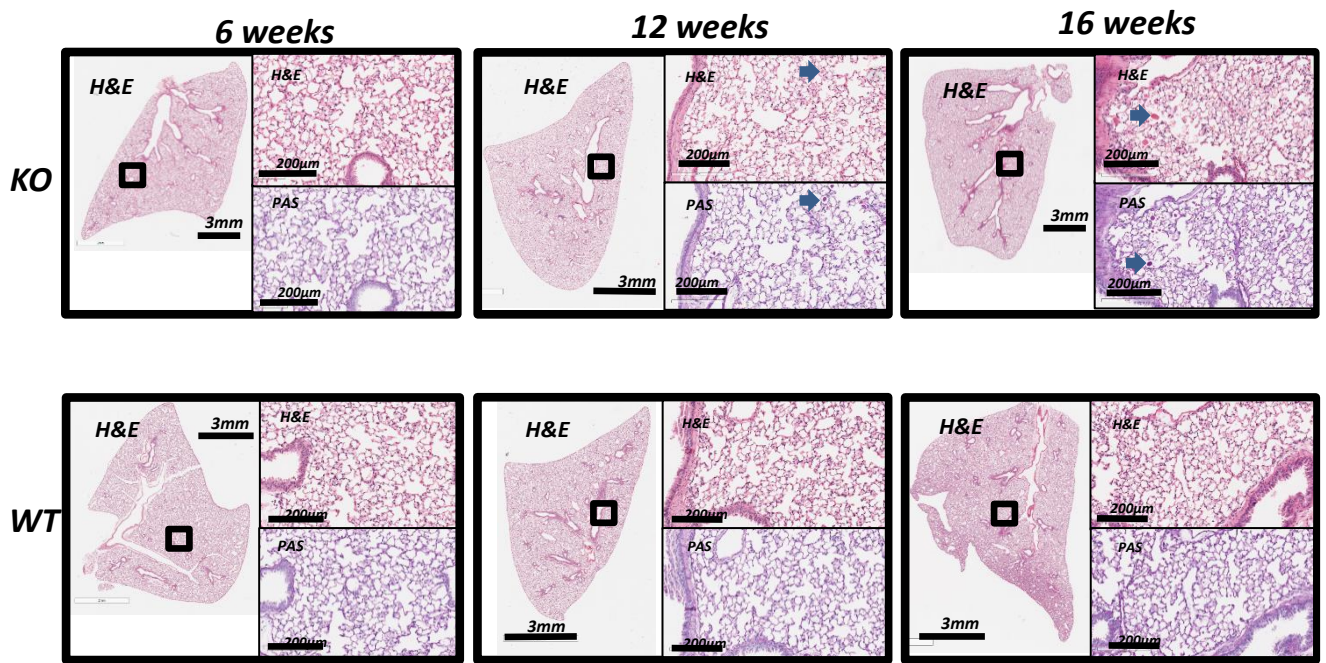


Figure 3B

Lungs from mice dosed with CAM-3003 for up to 24 weeks show no overt pathology

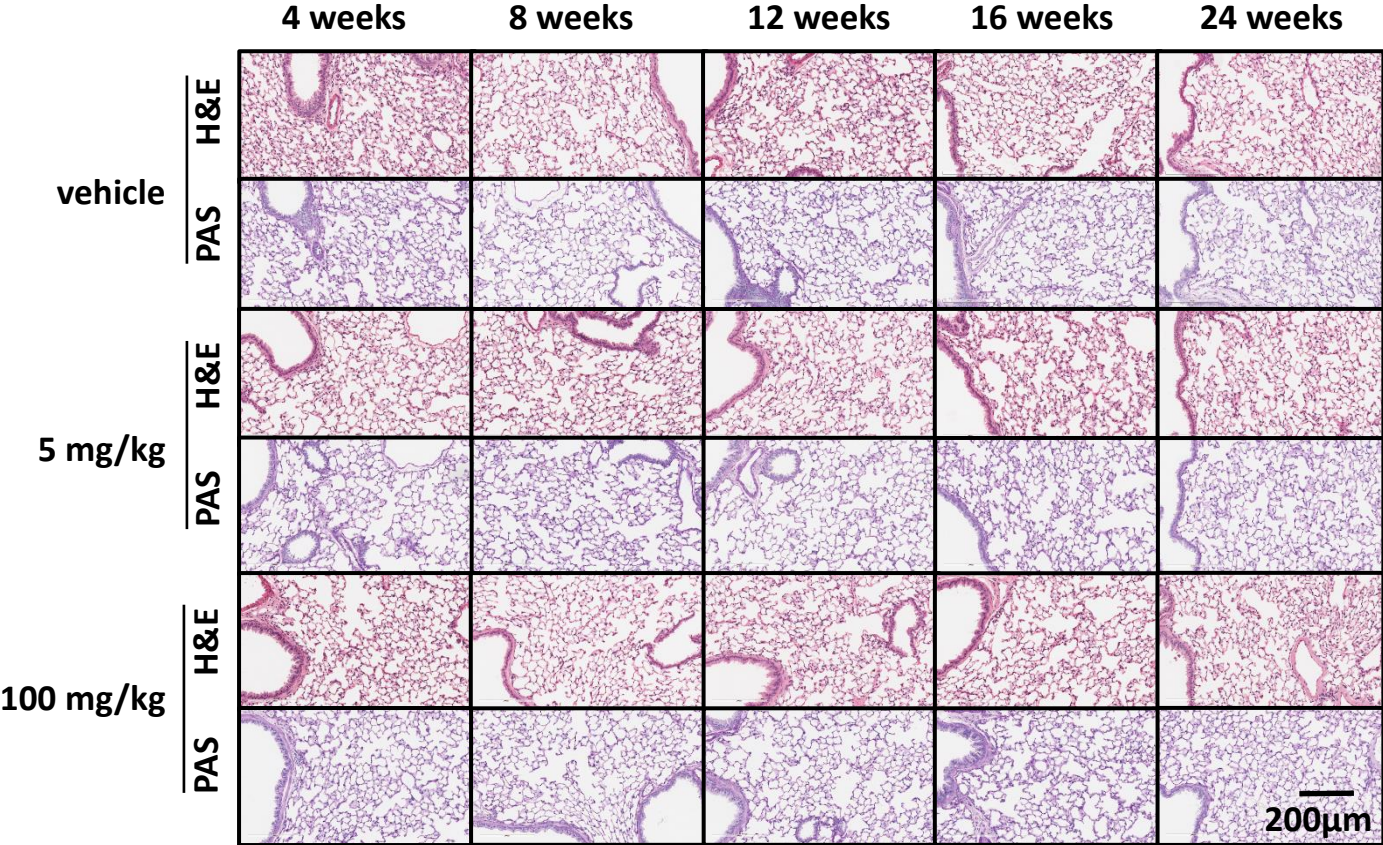


Figure 4.

**BALF PC recovered from CAM-3003 dosed mice compared with GMCSFR $\beta$  KO mice**

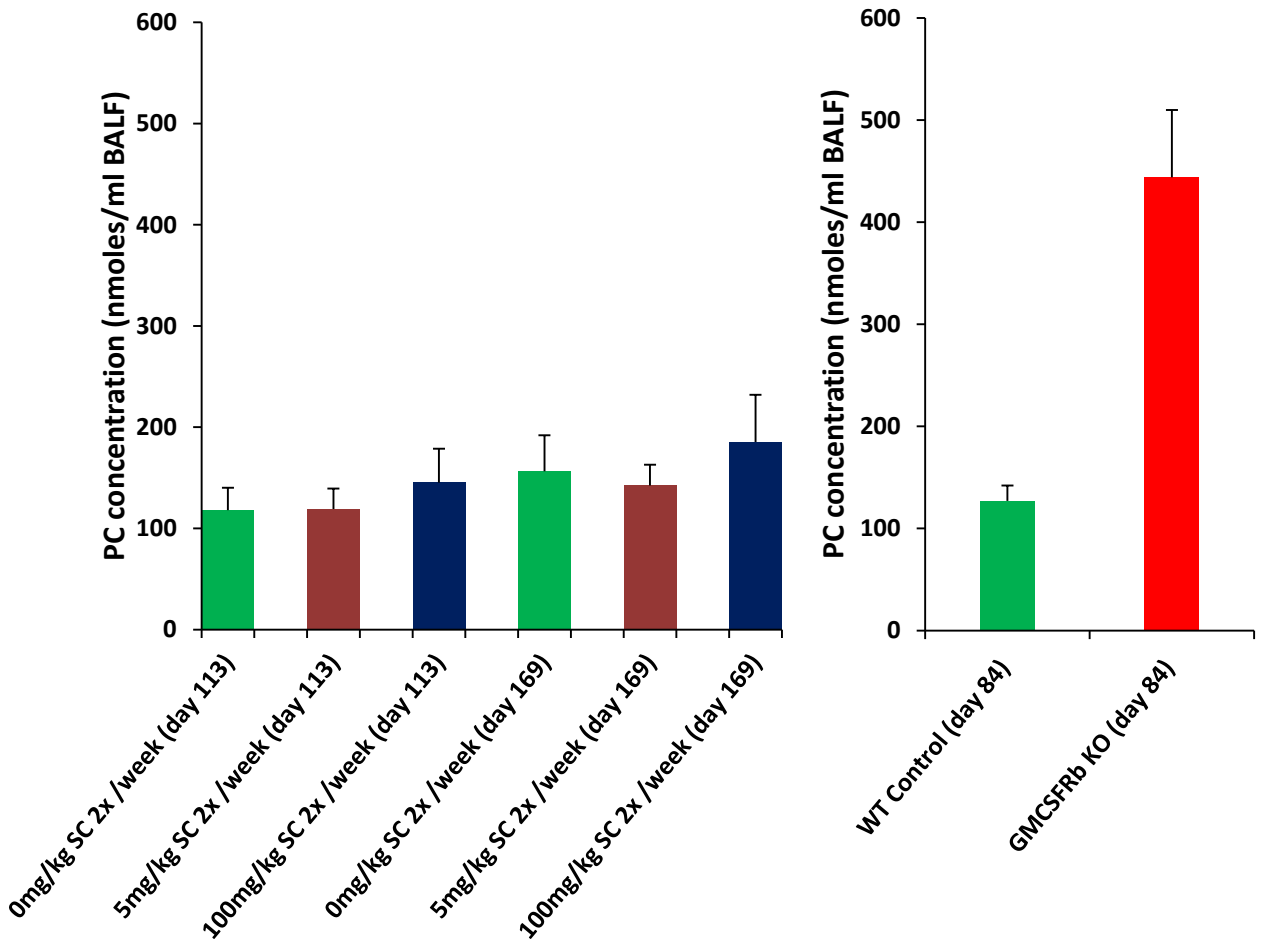


Figure 5.

PC molecular species compositions of lavaged lungs and corresponding BALF samples

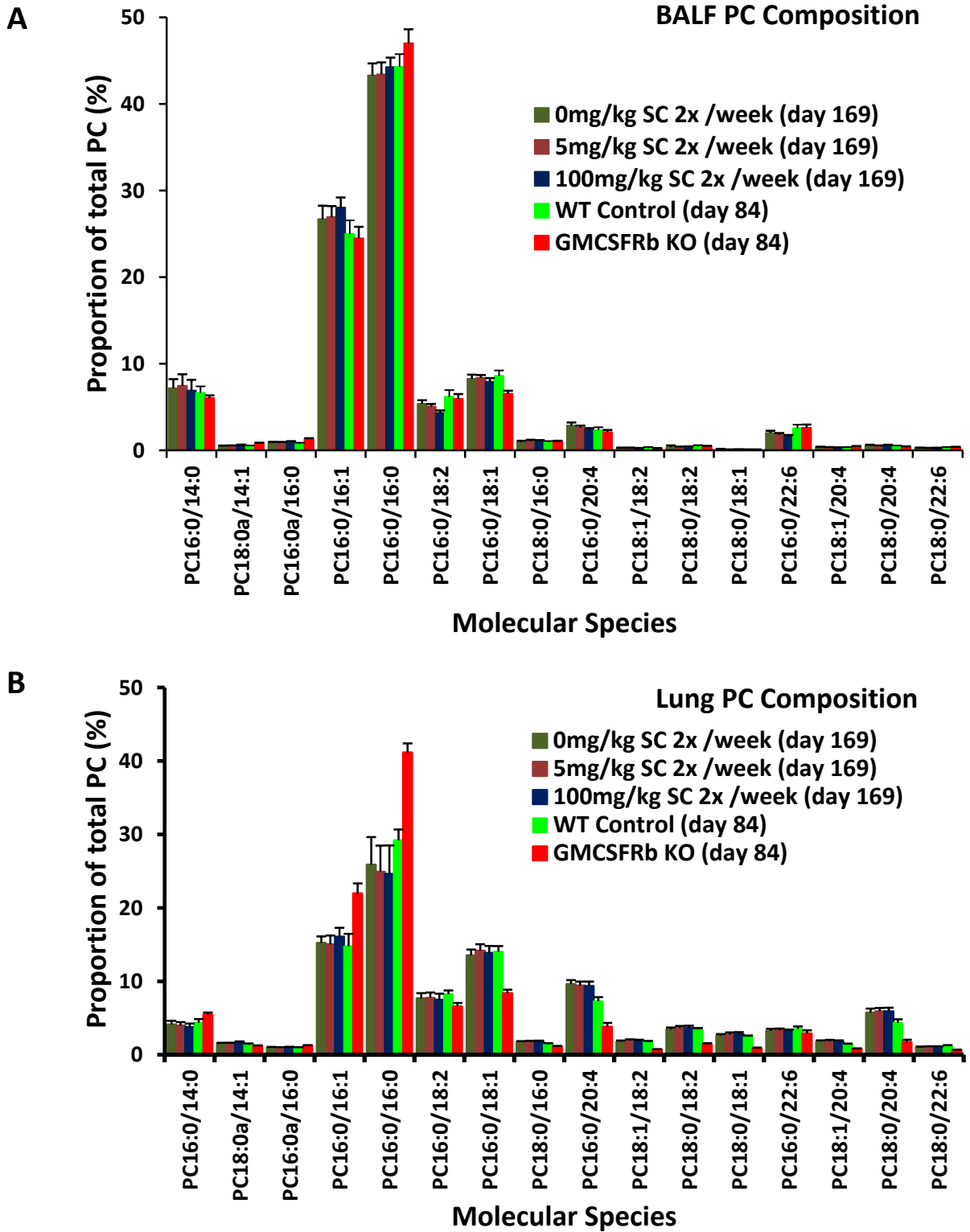


Figure 6

Incorporation of D9-choline into the lung PC of CAM-3003 dosed mice as a proportion of total PC

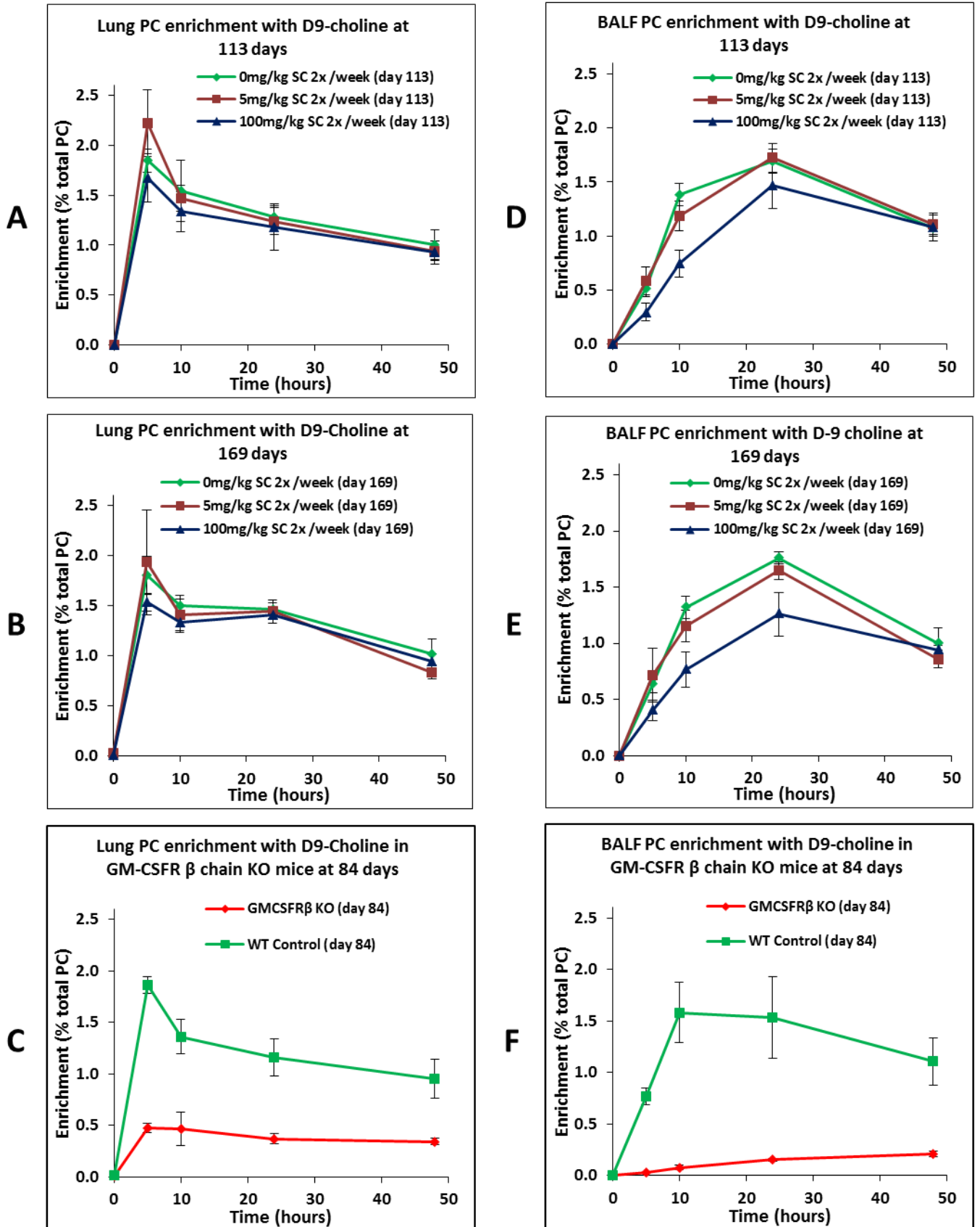
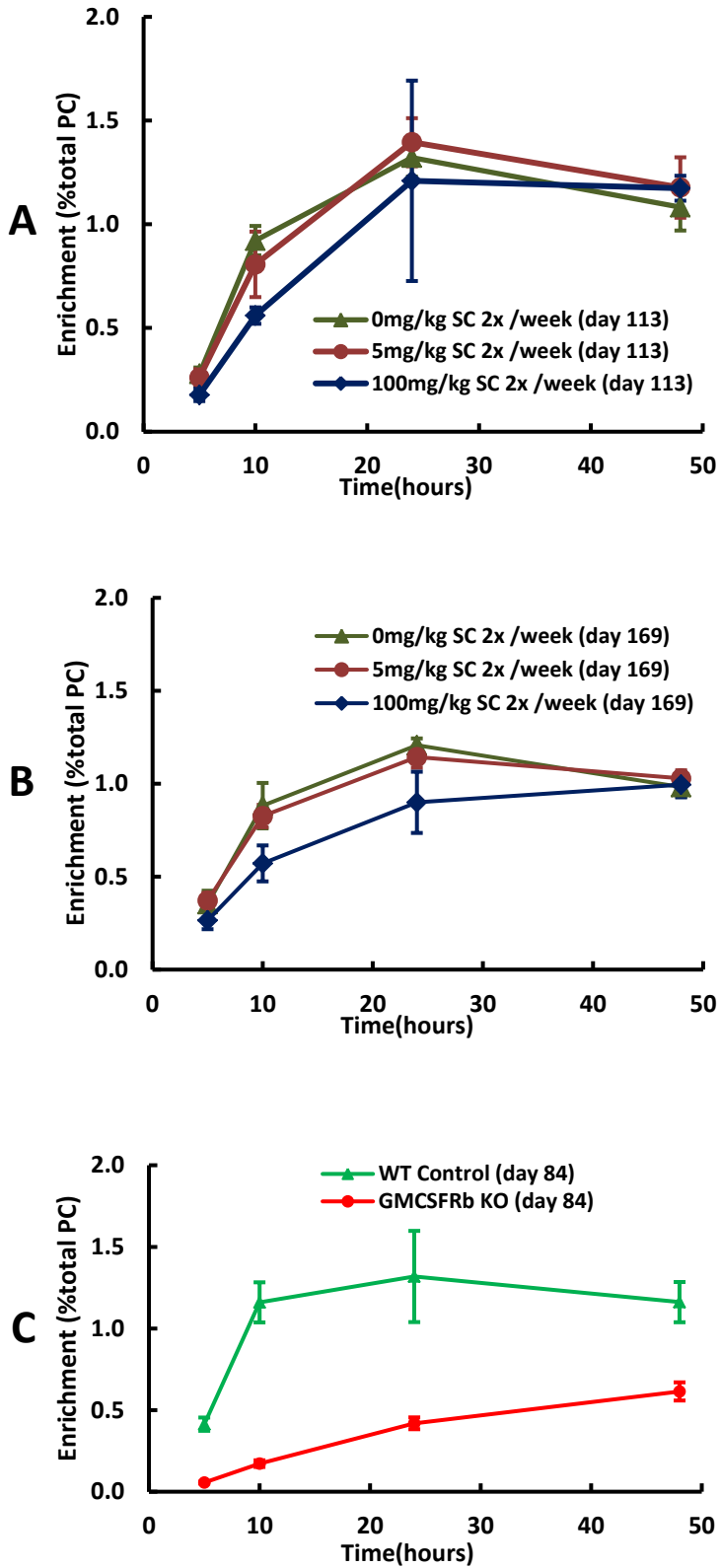


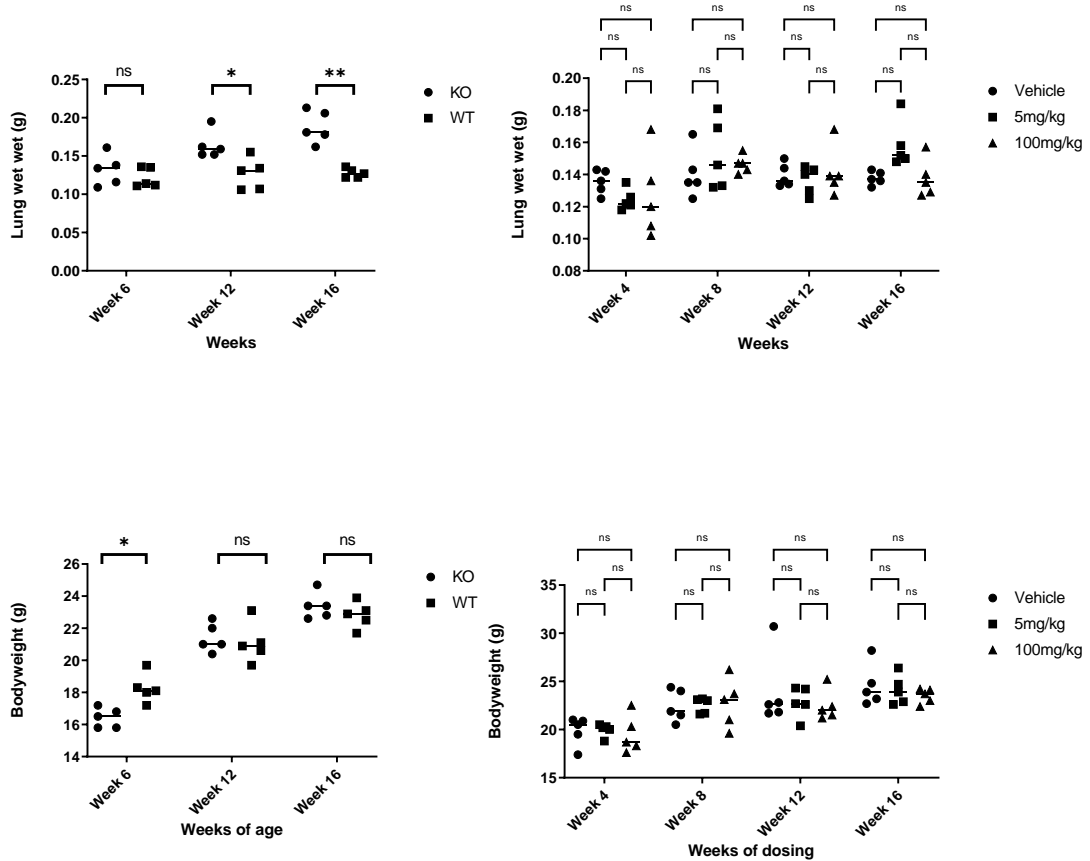
Figure 7

The ratio of BALF/Lung PC enrichment with *methyl-D<sub>9</sub>*-choline



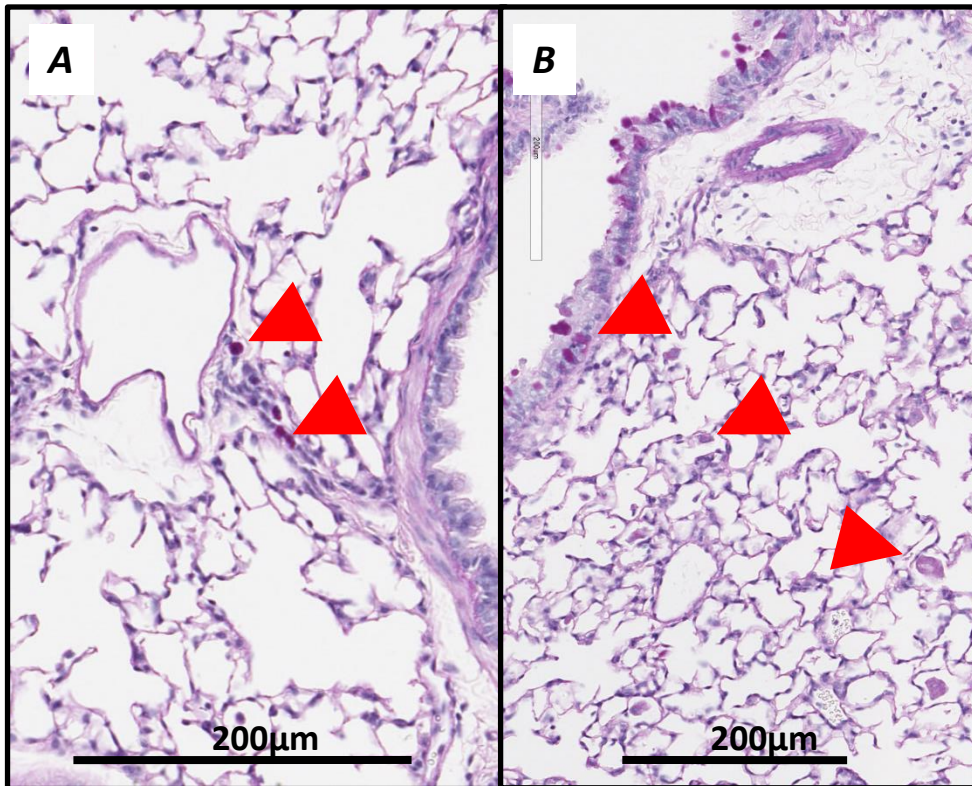
## Supplementary Figure 1

### Lung wet weight and bodyweight changes over time in GMCSFR $\beta$ KO mice, CAM-3003 dosed mice and controls



**Supplementary Figure 1.** Lung wet weight and bodyweight was recorded at termination in GMCSFR  $\beta$  KO (B6.129S1-Csf2rbtm1Cgb/J) and wildtype (C57Bl6J) cohorts (left panels), and CAM-3003 treated animals (right hand panels). Lung wet weight increases from 6 to 16 weeks in GMCSFR  $\beta$  KO mice relative to wildtype (Mann-Whitney 2-tailed t-test, \* $P < 0.05$ , \*\* $P < 0.01$ , ns - not significant). No difference in lung weight is observed between CAM-3003 treated and vehicle treated animals (2-way ANOVA followed by Tukey's multiple comparison test). A small difference in bodyweight at termination was seen at 6 weeks of age between the wild-type and GMCSFR  $\beta$  KO mice (Mann-Whitney 2-tailed t-test). No further significant differences in bodyweight at termination were observed between wild-type vs GMCSFR  $\beta$  KO or vehicle vs CAM-3003 treated cohorts (2-way ANOVA followed by Tukey's multiple comparison test).

High power images of lungs of CAM-3003 high dose animals



**Supplementary Figure 2.** Selected high power images of the lung parenchyma from animals receiving 100mg/kg CAM-3003, arrows show occasional PAS+ staining in macrophages, epithelium and alveoli with minimal pathology. Panel A – Mouse #94 showing PAS +ve macs Panel B – Mouse #96 showing PAS+ epithelium, slightly PAS+ mac and also some PAS+ material in alveoli

Supplementary Table 1

			Pathology endpoint (endpoint weeks of dosing or weeks of age for KO cohorts)						PK*	Lipid profiling endpoint (endpoint weeks of dosing or weeks of age for KO cohorts)				
			4	6	8	12	16	24		6	8	12	16	24
Dosing cohort	Genotype	Dose mg/kg												
	C57Bl6J (CRUK)	0	5	-	5	5	5	5		-	5	-	25	25
	C57Bl6J (CRUK)	5	5	-	5	5	5	5	42	-	5	-	25	25
	C57Bl6J (CRUK)	100	5	-	5	5	5	5	42	-	5	-	25	25
GMCSFR $\beta$ KO cohort	B6.129S1-Csf2rb <sup>tm1Cgb/J</sup> (Jax, USA)	-	-	5	-	5	5	-		5	-	25	5	
	C57Bl6J (Jax, USA)	-	-	5	-	5	5	-		5	-	25	5	

**Supplementary Table 1.** Table shows number of mice allocated to study groups and endpoints in the CAM-3003 treated and GMCSFR $\beta$  KO (B6.129S1-Csf2rb<sup>tm1Cgb/J</sup>) and wildtype (C57Bl6J) cohorts.